The Infrared Difference Dust Index

Michel Legrand

Bldg P5, Dept of Physics, LOA – University of Lille, Villeneuve d´Ascq, France

michel.legrand@univ-lille.fr

Derived from *The Infrared Difference Dust Index: past, present and future* (Legrand et al., 2010).

Introduction

The Infrared Difference Dust Index (IDDI) derived from the Earth observation by means of the IR channel of Meteosat "First Generation" (MFG), is a daytime indicator of dust over land. It can be expressed as a satellite radiance or brightness temperature deficit, or contrast (King et al., 1999) due to dust presence, especially effective over arid and semi-arid surfaces.The IDDI is thus relevant to study the emission of dust particles from desert sources, and their transport.

An upgraded IDDI version has been initiated in the 2000s and finalized after 2010 and is currently implemented (the former IDDI version has been described in Legrand et al., 2001). A 24-year IDDI database over Africa (1982-2006) has been realized with Meteosat 2 to 7 at 0°. A 19-year IDDI database over SW Asia (1998-2017), obtained successively from Meteosat 5 located at 63° E, then from Meteosat 7 located at 57° E, has been added to the database over Africa.

Hereafter are recalled the main physical bases of IDDI. The upgraded IDDI algorithm is briefly presented. Some results – realized or suggested – are shown in relation with various applications and researches using the data from the new base.

A regional African dust storm visualized using IDDI

Example of the evolution of the major Saharan dust event of 7 to 10 March 2006, at its outbreak during the day of 7 March at 9, 12 and 15 UTC. The IDDI color scale (0 – 25 K, at right side of the figure) indicates the dust thermal contrast – i.e. the brightness temperature deficit (in K) – due to the presence of dust. The dust front appears distinctly, streaching from the Sinai (NE Egypt) to the Atlantic coast nearby Dakar (Senegal). Measurements from Meteosat 7, at 0°.
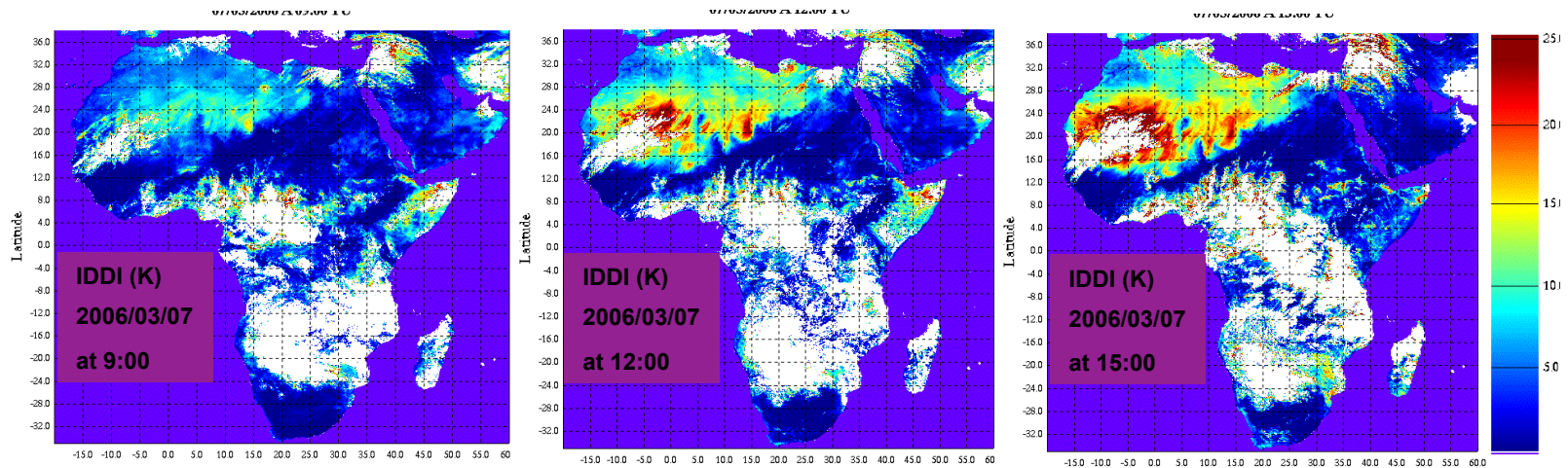
from Legrand et al., 2009

Thermal infrared remote sensing basics with MFG

Remote sensing with terrestrial radiation :

Source = Earth surface

Satellite observation of atmosphere **by transmission**

is like

Sun photometry :

Source = Sun surface

Photometer observation of atmosphere **by transmission**

but is different of

Remote sensing with solar radiation :

Source = Sun surface

Satellite observation of atmosphere **by reflection**

MFG: IR channel
10.5-12.5 µm (TIR)
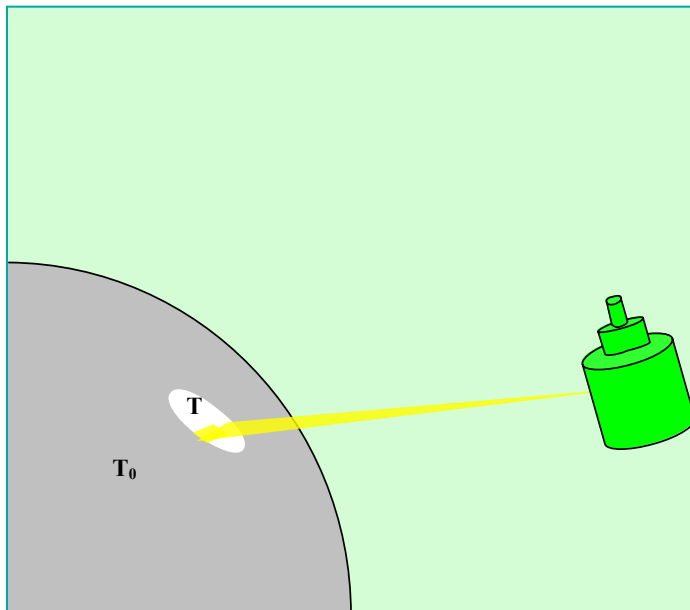plus **VIS channel**
for the **Cloud mask**

Geostationary

What is measured?
Radiance (TIR)
Brightness temperature

Physical bases :
Contrast of an opaque object

In the thermal infrared (TIR), a real surface is never perfectly black: instead, it is characterized with an emissivity ε: $0 < \varepsilon < 1$.

- Contrast definition (with the radiances):

$$C = L - L_0$$

- Radiance L and brightness temperature T^* are related by:

$$L = B(T^*)$$

B is the blackbody function.

With the assumptions:

- **H1**: object (opaque) and Earth surface are black in the TIR;
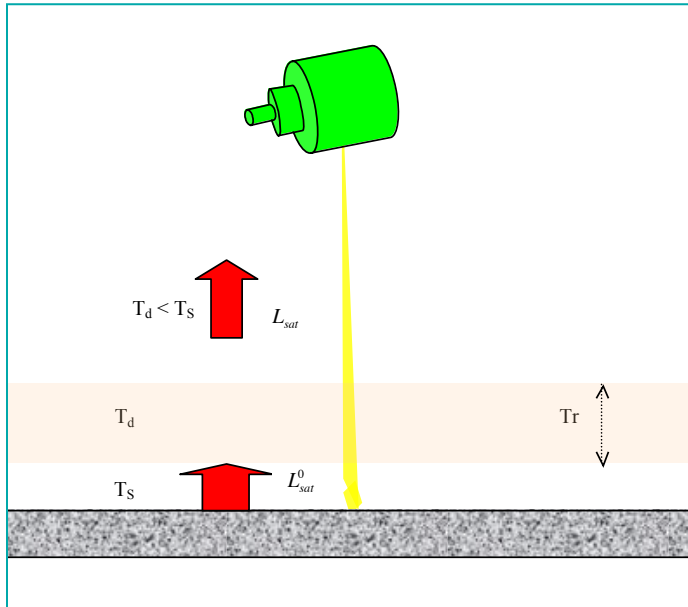
- **H2**: no atmosphere: $T^* = T$

- T is the surface (skin) temperature.

- A definition of the object contrast can also be given with the brightness temperature (BT):

$$C = B(T) - B(T_0)$$

$$C_T = T^* - T_0^* = T - T_0$$

Thermal contrast of a dust layer over a hot surface

$T_d < T_S$

L_{sat}

T_d

T_S

Tr

L_{sat}^0

Estimating the dust impact (i.e. contrast) using simplifying assumptions, needs values from the diagram above for temperatures T_S, T_d and dust layer transmittance Tr (or TIR dust layer optical depth δ).

Let us consider this question (right column) for mineral dust over an arid area (Sahara, Sahel in the dry season).

- • Dust layer: semi-transparent absorbing, scattering and emitting object.

- • Simplifying assumptions:

- • **H1**: absorbing gases not considered

- • **H2**: surface assumed black, at temperature T_s

- • **H3**: dust layer assumed non scattering and isothermal at T_d, with transmittance Tr

- • Radiance outgoing to space is

- without dust: - with dust:

$$L_{sat}^0 = B(T_S)$$ $$L_{sat} = Tr.B(T_S) + (1 - Tr).B(T_d)$$

- • Dust impact (contrast) obtained by difference is:
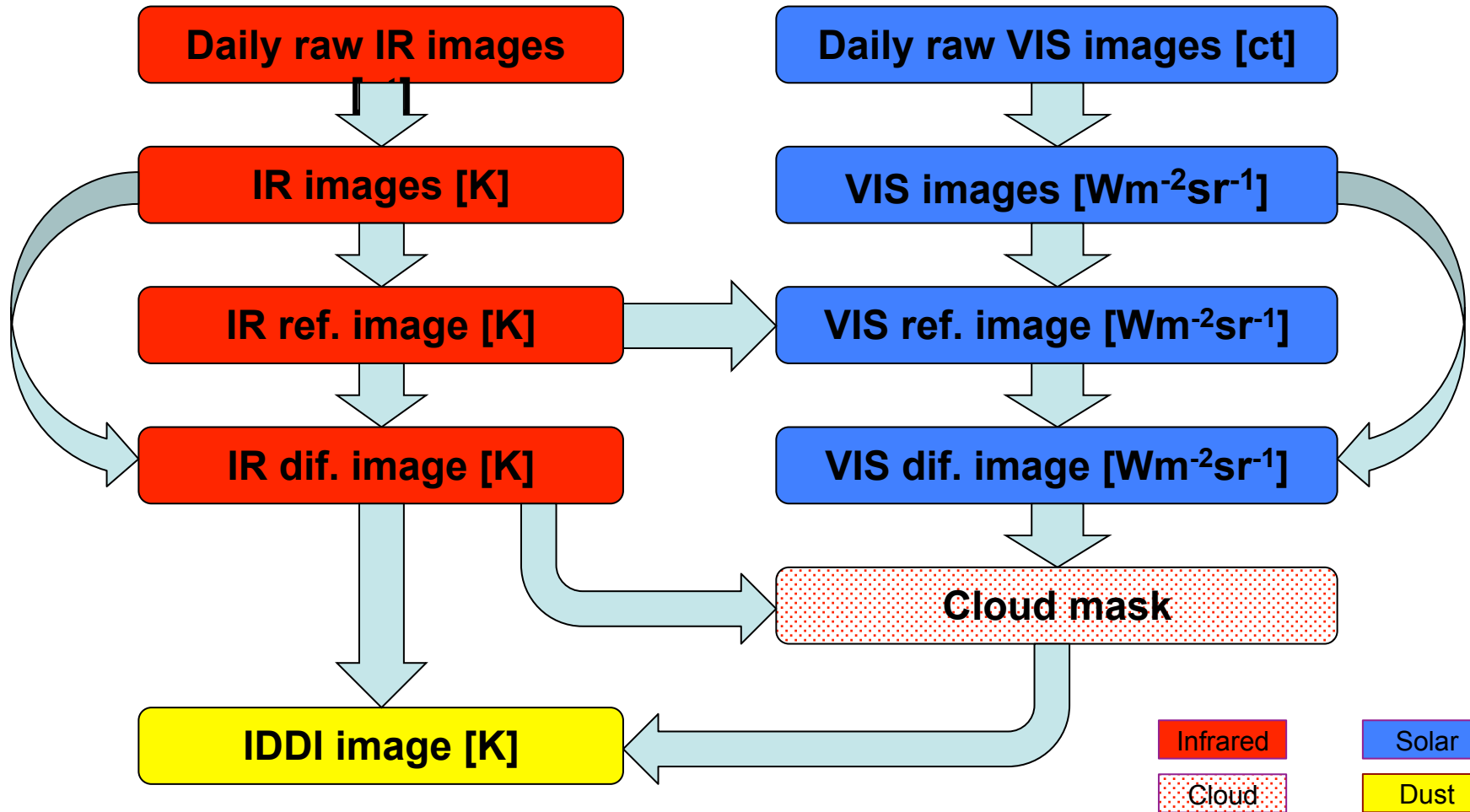
$$\Delta L_{sat} = (1 - Tr).[B(T_d) - B(T_S)]$$

- • The radiance contrast (defined as > 0) is $|\Delta L_{sat}|$.

- • The BT contrast (defined as > 0) is:

$$C_T = |T_d * - T_s|$$

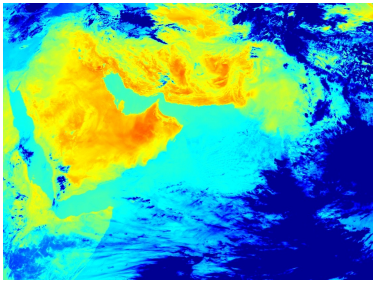- • It is maximum for $Tr = 0$, with the value $|T_d - T_s|$.

New IDDI algorithm scheme (BT in K)

(for the creation of the reference and difference images, consider the former algorithm in Legrand et al., 2001)
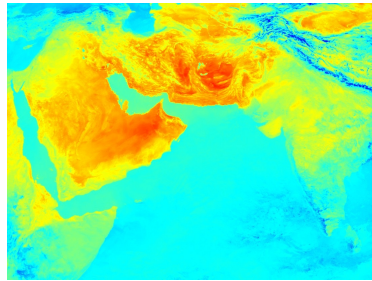

Daily raw IR images [ ]

IR images [K]

IR ref. image [K]

IR dif. image [K]

IDDI image [K]

Daily raw VIS images [ct]

VIS images [Wm^{-2}sr^{-1}]

VIS ref. image [Wm^{-2}sr^{-1}]

VIS dif. image [Wm^{-2}sr^{-1}]

Cloud mask

Infrared Solar

Cloud Dust

IDDI algorithm intermediate products
(MFG 5 - 63°E – 10/06/1999 @ 8:00 UTC)
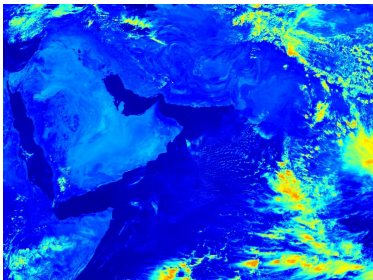
Daily IR
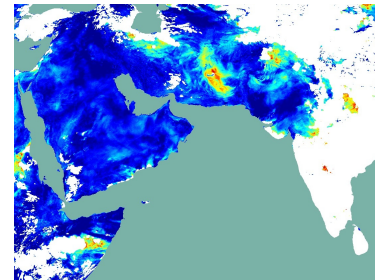
IR reference
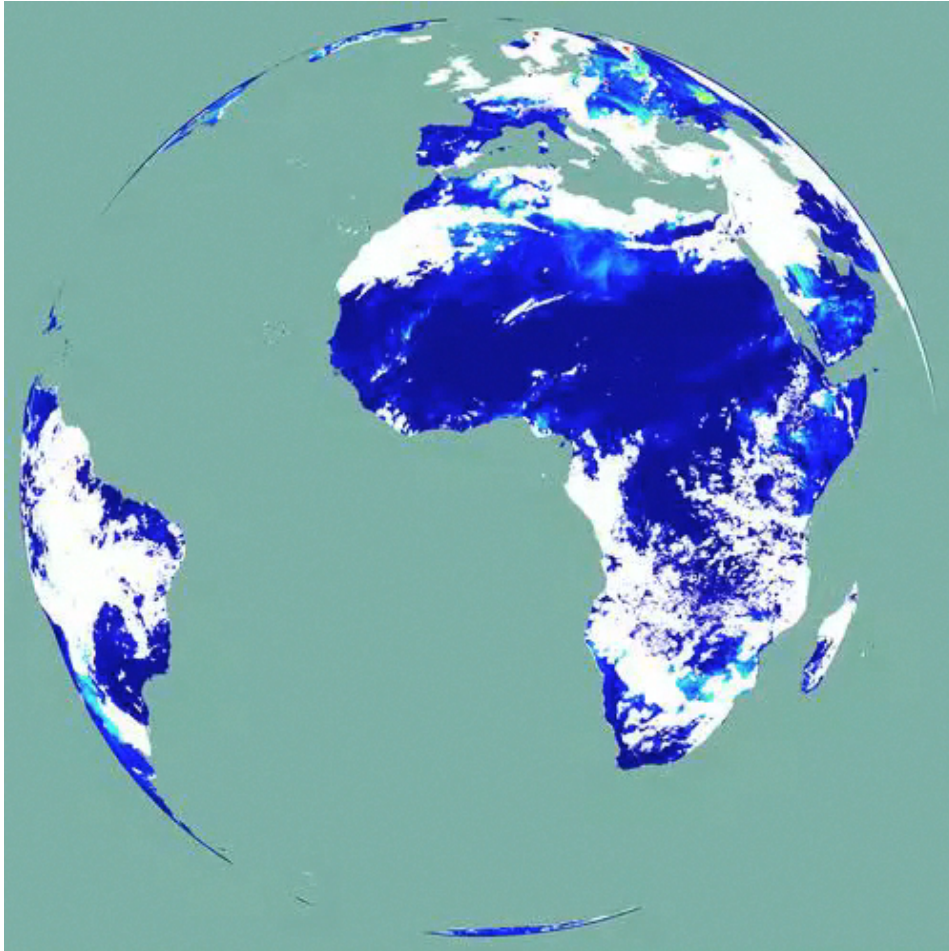
IR difference
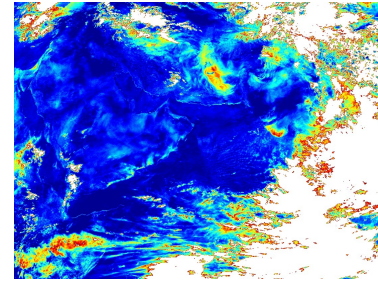
Daily VIS

VIS reference

IDDI

Increasing IR BT and VIS radiance from blue to red (BT scale from 250K to 340K).
Increasing IR BT-differences and IDDI from blue to red (IDDI scale from 0 to 25 K).

Sources activity in Africa (February 1992)

**Video QuickTime:
"sources_1992-02-22.mov"
(external to the diaporama).**

Note the presence of stationary
dust plumes anchored to sources
of the "Sahelian belt" in the animation.
The sources are activated by the surface
wind associated to the proximity of a
pressure low.

Dust transport over Africa toward Atlantic Ocean (July-August 1985)
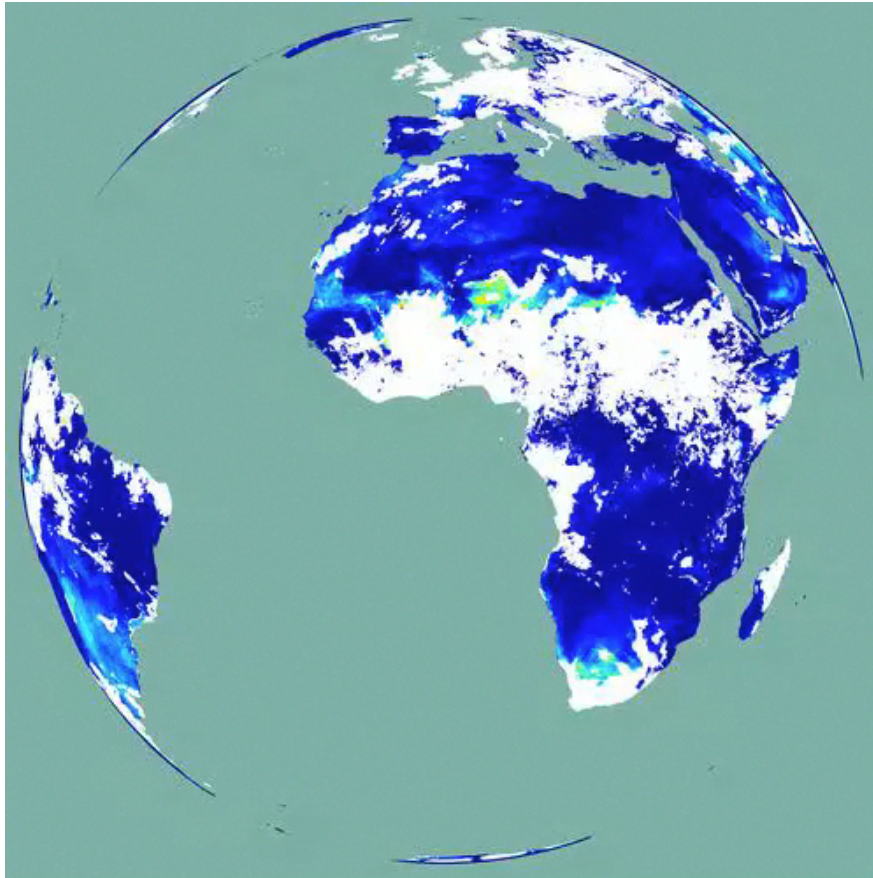
**Video QuickTime:
"transport_1985-07-11.mov"
(external to the diaporama).**

Dust plumes are emitted from the sources of the "Sahelian belt" and are transported westward and expelled over the tropical Atlantic. The phenomenon is repeated with an approximate periodicity of a few days, giving rise to a real "dust-train". This animation created with following daily IDDI images covers a period of 7 weeks.

Generation of dust storms from the Sistan source, Iran – 10-15 July, 2003
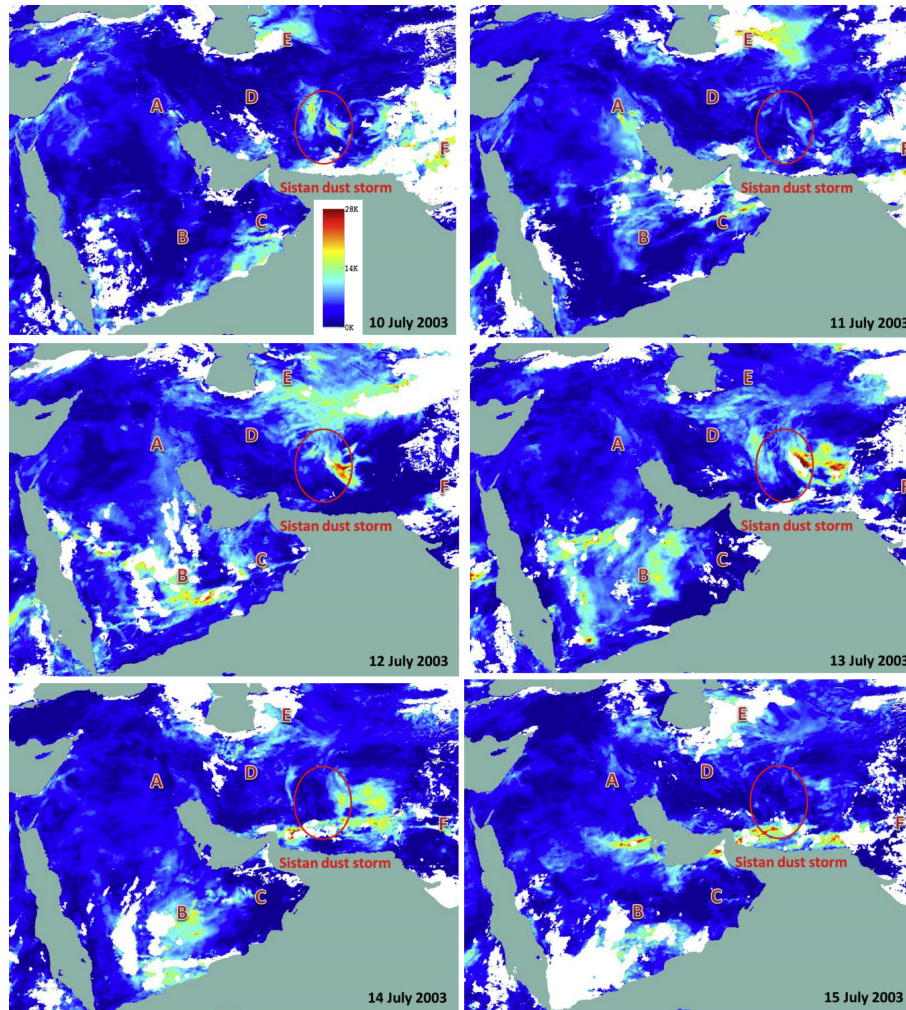
The Sistan source is located in Iran, around the Hamoun lakes, near its borders with Pakistan and Afghanistan. Occurrence of completely dried lakebeds during summers of the driest periods, leads to strong dust storms (visibility range ≤ 1 km) in the June-September season, making this source a prominent hotspot in the region.

The figure shows successive dust outbreaks arising from this source, under the Levar (north wind) effect, with IDDI values exceeding 30 K.

from Rashki et al., 2015

Mean monthly IDDI: all days – dust storm days Sistan, Summer (JJAS) 2001-2006
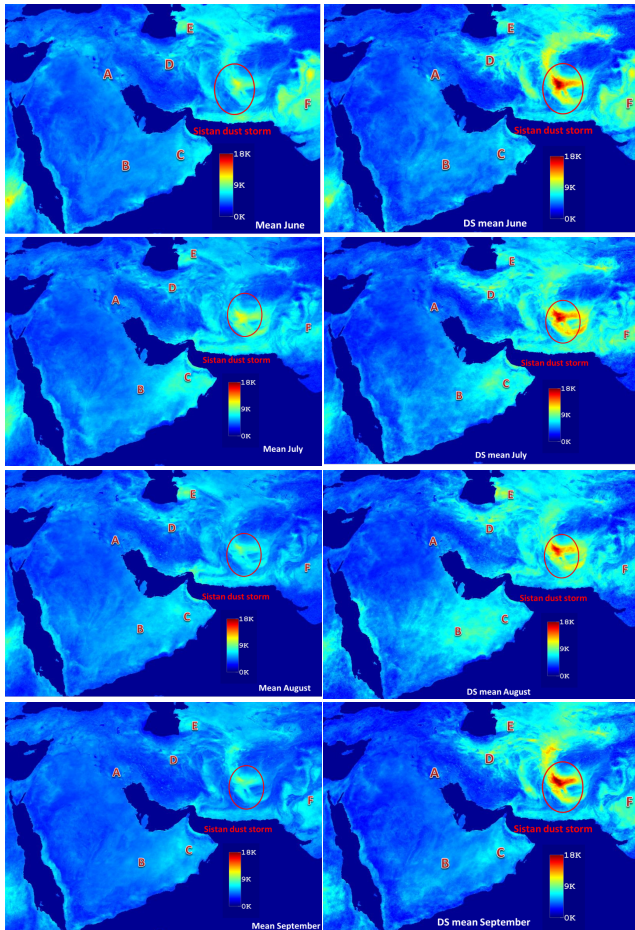
These images show monthly means over SW Asia derived from the daily IDDI images. Such monthly means are suitable to reveal the sources location. The left column shows the monthly means from all days in the month (JJAS). The right column shows the monthly means using only the days with a dust storm (visibility ≤ 1 km) detected at the station of Zabol, Sistan, Iran. This filtering keeps only the very dusty days at Zabol, which provides a much more distinct description of the Sistan source (right column) than the simple monthly mean (left column).

from Kaskaouti et al., 2014

IDDI against visibility range: dust storm days Jun-Sep 2001-2006 at Zabol (Sistan, Iran)

Relation IDDI – Visibility during summer dust storms at Zabol (Sistan, Iran) 2001-2006
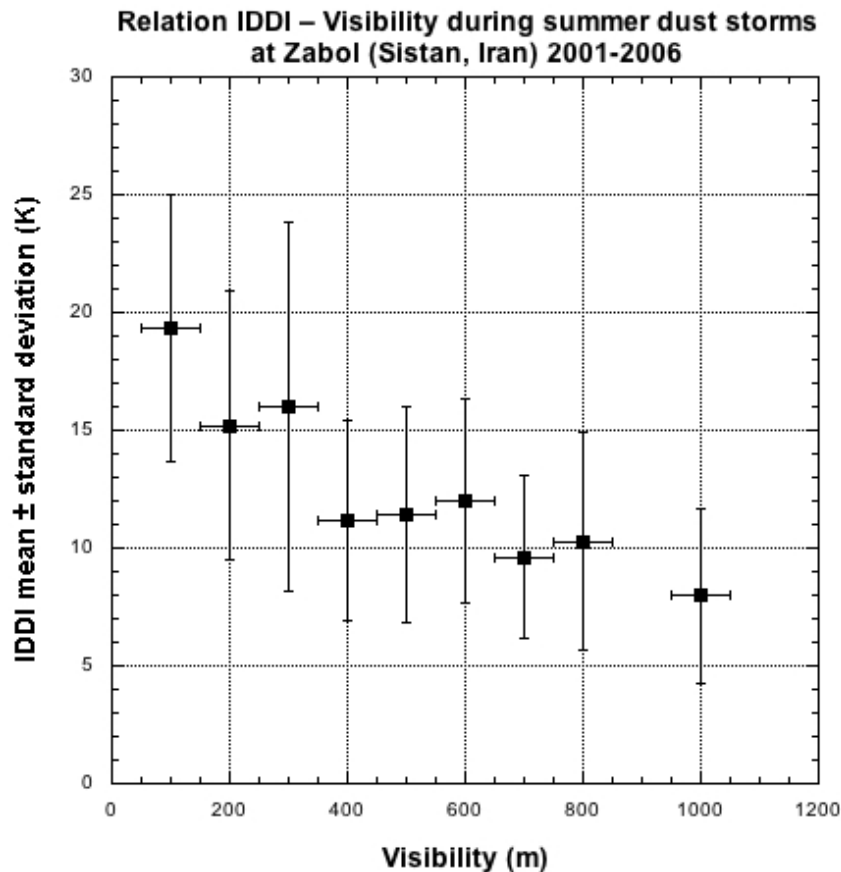
Horizontal visibility range is a reliable index of dust haze concentration (N'tchayi et al., 1994). So, a visibility range not exceeding 1 km (in dry air), defines a dust storm (WMO). In the figure are plotted the mean IDDI values for visibility bins 100 m wide covering the range from 0 to 1 km (no bin at 900 m). The vertical bars are for ± σ (sta.dev.); the horizontal bars are for ± 50 m (Zabol, Sistan, June to September, 2001-2006).

AERONET AOD @ 1020 nm against IDDI:
# all days 12-13 UTC – 2003-2006, Agoufou (Mali)

Relation AERONET AOD @ 1020 nm – IDDI
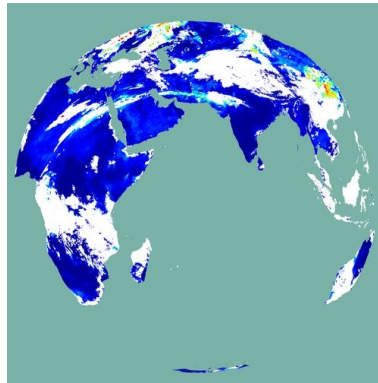all days - 2003-2006 (Agoufou, Mali)
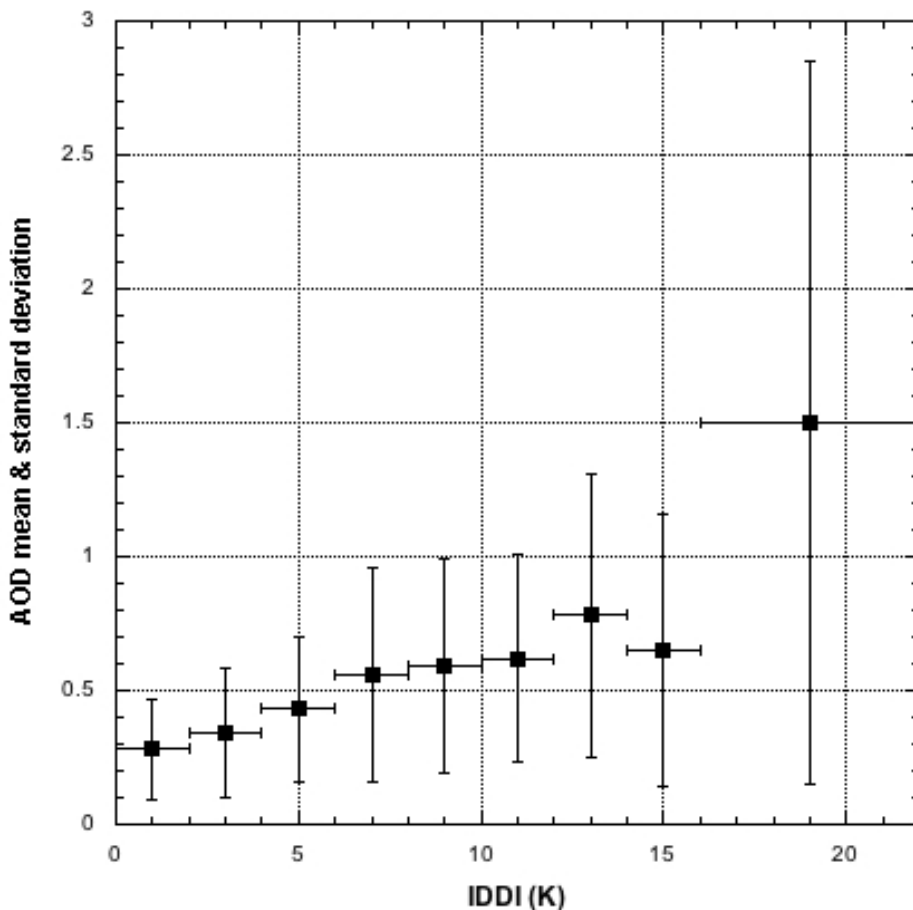
Agoufou is an AERONET station near the village of the same name (south Mali, Sahel), where AOD at 1020 nm is measured with a photometer.
Increasing IDDI corresponds to increasing AOD. Note that a more direct relation would be expected, using a TIR AOD, instead of the near-infrared AOD from AERONET.

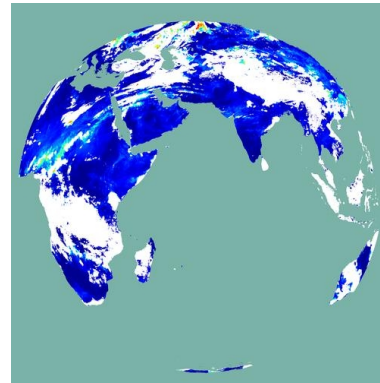# A case of IDDI-revealed low-level dusty jet
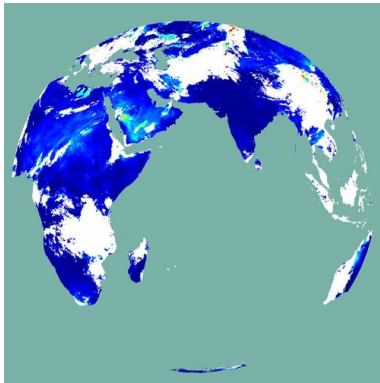
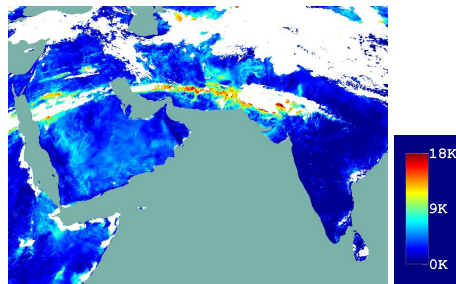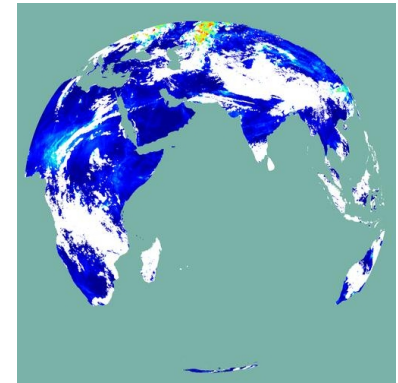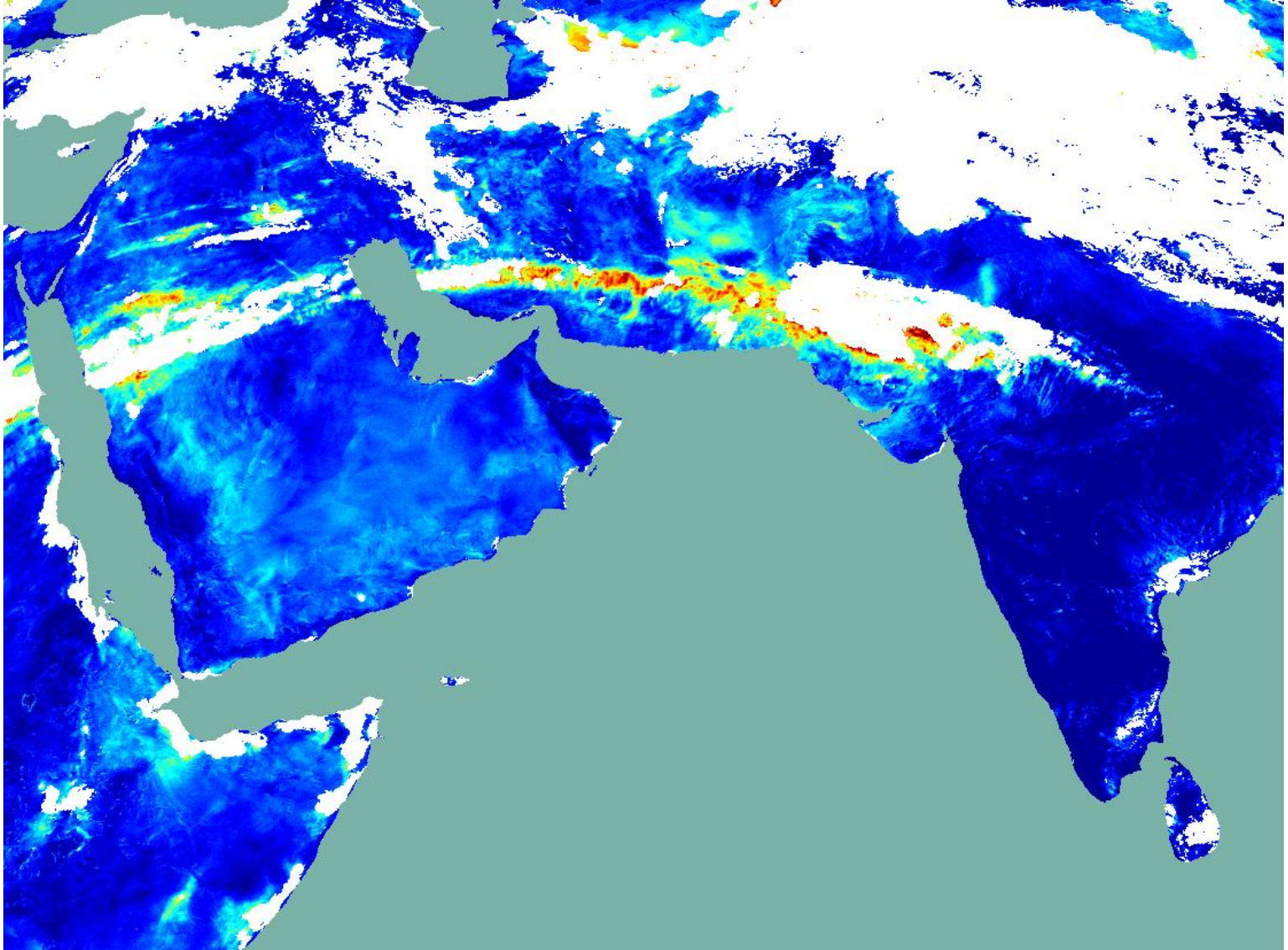2000-01-30   2000-01-31   2000-02-01   2000-02-02

The elongated structure observable over Asia and Africa, above, aside and in the next slide, is obviously an atmospheric jet vizualized by the presence of dust.
Further investigations on this phenomenon would be welcome.

A case of IDDI-revealed low-level dusty jet

State of the art and projects for IDDI
Available database

- The IDDI product proved to be useful in determination of dust sources location and seasonal activity (Brooks and Legrand, 2000; Leon and Legrand, 2003; Deepshikha et al., 2003a;b), in the physics of dust emission with respect to the surface properties (Chomette et al., 1999; Marticorena et al., 1997; 1999; 2004), for description of dust transport (Petit et al., 2005), for dust mineral origin and composition (Caquineau et al., 2002), for dust activity connection with the climate (Kaskaoutis et al., 2014; 2015; 2016; 2017; Rashkhi et al., 2015) and for dust meteorological forecasting (Hu et al., 2008).

- As to the prospects, the MFG at 0° archive from 1982 to 2006 is planned to be extended beyond 2006 through MSG data, which needs adaptations of spectral channels and of spatial resolution, different between MFG and MSG. The same operation could be done for the archive for SW Asia where a MSG satellite has been substituted to Meteosat 7 in 2017.

- These evolutions would enable to progress in the knowledge of the topics of concern such as the climatology of desert sources, the study of dust emission and transport, the relations between dust and clouds, the long-term evolutions of heating/cooling and of drought/ vegetation recovery; this list being only indicative. Within these studies, the long-term (decennial) evolutions can been accessed. More generally, the IDDI images are intended to be used by our scientific community for every subject to which it would be of interest. For this, a website is being created to access archived imageries.

- In this initial step, jpeg IDDI images can be viewed over the above-mentioned periods.

References

- Brooks N.P.J., Legrand M. (2000), in *Linking climate change to landsurface change*, Chapter 1, 1-25, Kluwer Academic Publishers.
- Caquineau S., Gaudichet A., Gomes L., Legrand M. (2002), *J. Geophys. Res., 107*, doi.10.1029/2000JD000247.
- Chomette O., Legrand M., Marticorena, B. (1999), *J. Geophys. Res., 104*, 31207-31215.
- Deepshikha S., Satheesh S.K,. Srinivasan J. (2003), *Ann. Geophys., 24*, 37-61.
- Deepshikha S., Satheesh S.K., Srinivasan J. (2003), *Ann. Geophys., 24*, 63-79.
- Hu X.Q., Lu N.M., Niu T., Zhang P. (2008), *Atmos. Chem. Phys., 8*, 1649-1659.
- Kaskaoutis D.G., Rashki A., Houssos E.E., Mofidi A., Goto D., Bartzokas A., Francois P., Legrand M. (2014), *Clim. Dyn.*, *45*, 407-424.
- Kaskaoutis D.G., Francois P., Dumka U., Houssos E., Legrand M. (2015), *Aeolian Res.*, 83-97.
- Kaskaoutis D.G., Houssos E.E., Rashki A., Francois P., Legrand M., Goto D., Bartzokas A., Kambezidis H.D., Takemura T. (2016), *Glob. Planet. Change*, 137, 10-23. doi.org/10.1016/j.gloplacha.2015.12.011.
- Kaskaoutis D.G., Rashki A., Houssos E.E., Legrand M., Francois P., Bartzokas A., Kambezidis H.D., Dumka U.C., Goto D., Takemura T. (2017), *Int. J. Climatol.*, DOI : 10.1002/joc.5053.
- King M.D., Kaufman Y.J., Tanre D., Nakajima T. (1999), *Bull. of the Am. Met. Soc., 80*, 2229-2259.
- Legrand M., Plana-Fattori A., N'doume C. (2001), *J. Geophys. Res., 106*, 18251-18274.
- Legrand M., Francois P., Nakes M.T. (2009), communication in *African Monsoon Multidisciplinary Analyses. Third International Conference. Ouagadougou, Burkina Faso, 20-24 July 2009*.
- Legrand M., Chiapello I., Francois P., Nakes M.T. (2010), invited conference in the Colloquium *Les Satellites Grand Champ pour le suivi de l'environnement, des ressources naturelles et des risques. Univ. B. Pascal; Clermont-Ferrand, 21-23 Jan. 2010*.
- Leon J.-F., Legrand M. (2003), *Geophys. Res. Lett.*, *30(6)*, 1309, doi.10.1029/ 2002GL016690.
- Marticorena B., Bergametti G., Aumont B., Callot Y., N'doume C., Legrand M. (1997), *J. Geophys. Res., 102*, 4387-4404.
- Marticorena B., Bergametti G., Legrand M. (1999), *Contr. Atmos. Phys., 72*, 151-160.
- Marticorena B., Chazette P., Bergametti G., Dulac F., Legrand M. (2004), *Int. J. Remote Sensing, 25*, 603-626.
- Petit R.H., Legrand M., Jankowiak I., Molinie J., Mansot J.L., Marion G., Asselin de Beauville C. (2005), *J. Geophys. Res.*, *110*, doi.10.1029/2004JD004748.
- Rashki A., Kaskaoutis D.G., Francois P., Kosmopoulos P.G., Legrand M. (2015), *Aeolian Res.*,*16*, 35-48. doi.org/10.1016/j.aeolia. 2014.10.003.